

Synthesis and morphological control of rare earth oxide nanoparticles by solvothermal reaction

Shu Yin · Shingo Akita · Makoto Shinozaki ·
Ruixing Li · Tsugio Sato

Received: 27 October 2006 / Accepted: 20 July 2007 / Published online: 27 September 2007
© Springer Science+Business Media, LLC 2007

Abstract Eu doped Y_2O_3 and some kinds of other rare earth oxides nanoparticles such as Er_2O_3 , Nd_2O_3 , Ho_2O_3 , Lu_2O_3 , and Dy_2O_3 were prepared by a simple co-precipitation-solvothermal treatment-calcination process, where the co-precipitated amorphous hydroxide precursors obtained by adding rare earth nitrate solutions in ammonia solutions were heated in solvents such as water, alcohols and glycols, followed by calcination in air. The morphology of rare earth oxide particles strongly depended on the solvothermal reaction medium but not related to the kind of rare earth oxide. The powders prepared in water and ethanol possessed nanowire structure, where the aspect ratio of powder treated in water was higher than that in ethanol. The powders prepared by co-precipitation-solvothermal treatment-calcination process using ethylene glycol consisted of near-spherical nanoparticles whereas that prepared by conventional co-precipitation-calcination method consisted of hardly agglomerated submicron particles. The nanoparticles of Eu^{3+} doped Y_2O_3 prepared by co-precipitation-solvothermal treatment-calcination process showed similar intensity of photoluminescence with the submicron particles by co-precipitation-calcination process.

Introduction

Eu^{3+} doped Y_2O_3 , $Y_2O_3:Eu$, and other rare earth oxides are the most important phosphors materials and expected wide

applications in novel type displays [1]. In order to realize high quality effect in display application and the miniaturization of electronic accessory, it is important to prepare well-crystallized luminescent materials with finer particle size and excellent photochemical properties. It has reported that phosphors materials with various morphologies such as hollow, porous, wire, rods, flakes, and spheres could be prepared by various methods such as spray method [2–5], anodic alumina oxide template method [6, 7], reverse micellar system [8, 9], and homogeneous precipitation method [10, 11], etc. Recently, the solvothermal method has become a promising method for the preparation of well-crystallized nano materials. In our previous research, it was found that nanosize TiO_2 , CeO_2/Y_2O_3 doped ZrO_2 , TiO_2-xN_y with excellent functional properties could be prepared by solvothermal reactions in various organic solvents [12–16]. In the present research, 3 mol.% Eu_2O_3 -doped Y_2O_3 nano particles [$Y_2O_3:Eu(3\text{ mol.}\%)$] and some other kind of rare earth oxides nanoparticles were prepared by the co-precipitation-solvothermal treatment-calcination process using aqueous, alcohols and glycols as reaction media, where the effect of the solvent on the morphologies and photoluminescence properties were investigated in detail.

Experimental

Sample preparation

After adding 150 mL of 0.2 M $Re(NO_3)_3$ aqueous solution in strongly stirred 200 mL of 4.5 M ammonia aqueous solution, the co-precipitated powders were washed with distilled water and respective organic solvents three times, then introduced to an autoclave with an internal volume of

S. Yin (✉) · S. Akita · M. Shinozaki · R. Li · T. Sato
Institute of Multidisciplinary Research for Advanced Materials,
Tohoku University, 2-1-1, Katahira, Aoba-ku, Sendai 980-8577,
Japan
e-mail: shuyin@tagen.tohoku.ac.jp

100 mL together with 60 mL of solvents, followed by solvothermal treatment at 250 °C for 5 h. Pure water, ethanol, 1-propanol, butanol, and some kinds of ethylene glycols such as 1,2-propanediol (1,2-PG), 1,3-propanediol (1,3-PG), 1,3-butanediol (1,3-BG), 1,4-butanediol (1,4-BG), 1,5-propanediol (1,5-PG), 1,6-hexanediol (1,6-HG), and polyethylene glycol 200 (PEG with the polymerization degree of 200), etc. were used as solvothermal reaction media. The powder product was separated by centrifugation, washed with distilled water and acetone three times, then vacuum dried at 60 °C for 24 h. In order to obtain oxide powder with different crystallinity and particle size, the product was calcined at various temperatures for 1 h.

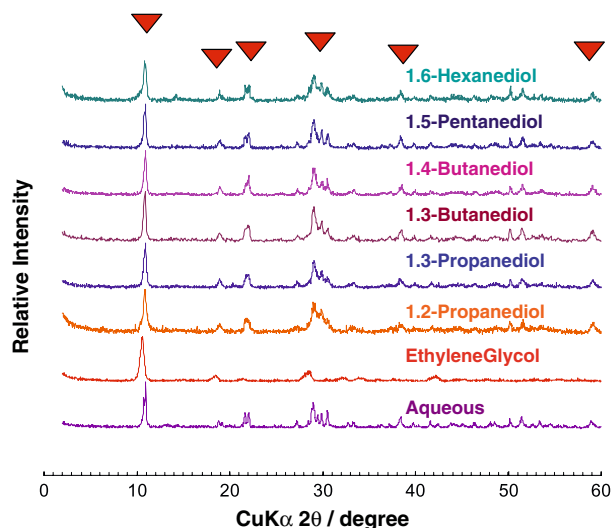
Analysis

The calcination temperature was determined by the result of thermo gravimetry-differential thermal analysis (TG-DTA, Rigaku TAS-200). The phase constitution of the product was determined by X-ray diffraction analysis (XRD, Shimadzu XD-D1) using graphite-monochromatized $\text{CuK}\alpha$ radiation. The morphology and particle size were observed by a transmission electron micrograph (TEM, JEOL JEM-2010). The photoluminescence spectra and intensity were measured by a spectrofluorophotometer (Shimadzu RF-5300P). The amount of residual carbon, hydrogen, and nitrogen elements were measured by a CHN analyzer (Yanako, MT-6).

Results and discussion

Figure 1 shows the XRD patterns of the powders prepared by solvothermal treatment in various solvents. Normally, different solvents used in solvothermal treatment affect the phase composition greatly during the solvothermal treatment [17]. However, in the present research, all the as-prepared samples by solvothermal treatment were identified as $\text{Y}_4\text{O}(\text{OH})_9(\text{NO}_3)$. There is no obvious variation in the type of phase formation with respect to the type of solvent used. All these products were treated by calcination in air at different temperatures. Figure 2 shows the TG-DTA profiles of the powders prepared by solvothermal treatments in water and ethylene glycol. The powder prepared by hydrothermal treatment showed two-steps weight loss, indicating that Y_2O_3 was produced by two-step dehydration of $\text{Y}_4\text{O}(\text{OH})_9(\text{NO}_3)$ during the calcination process. The first weight loss accompanied with the endothermic peak around 390 °C is related to the disengaging of NO_3^- from $\text{Y}_4\text{O}(\text{OH})_9(\text{NO}_3)$, the second weight loss accompanied with the endothermic peak around 480 °C is related to the dehydration to form Y_2O_3 . The weight loss determined by TG-DTA measurement agreed well with the calculated value for the formation of Y_2O_3 from $\text{Y}_4\text{O}(\text{OH})_9(\text{NO}_3)$. On the other hand, the powder prepared by solvothermal treatment in ethylene glycol showed some exothermic peaks probably caused by the combustion of the residual organic solvent, indicating the adsorption of ethylene glycol in the products. Although the detail was not clarified yet, it is suggested that the

Fig. 1 XRD patterns of the powders prepared by solvothermal treatment in (a) water [AQ], (b) ethylene glycol [EG], (c) 1,2-propanediol [1,2-PG], (d) 1,3-propanediol [1,3-PG], (e) 1,3-butanediol [1,3-BG], (f) 1,4-butanediol [1,4-BG], (g) 1,5-propanediol [1,5-PG], (h) 1,6-hexanediol [1,6-HG] at 250 °C for 5 h. ▼: $\text{Y}_4\text{O}(\text{OH})_9(\text{NO}_3)$



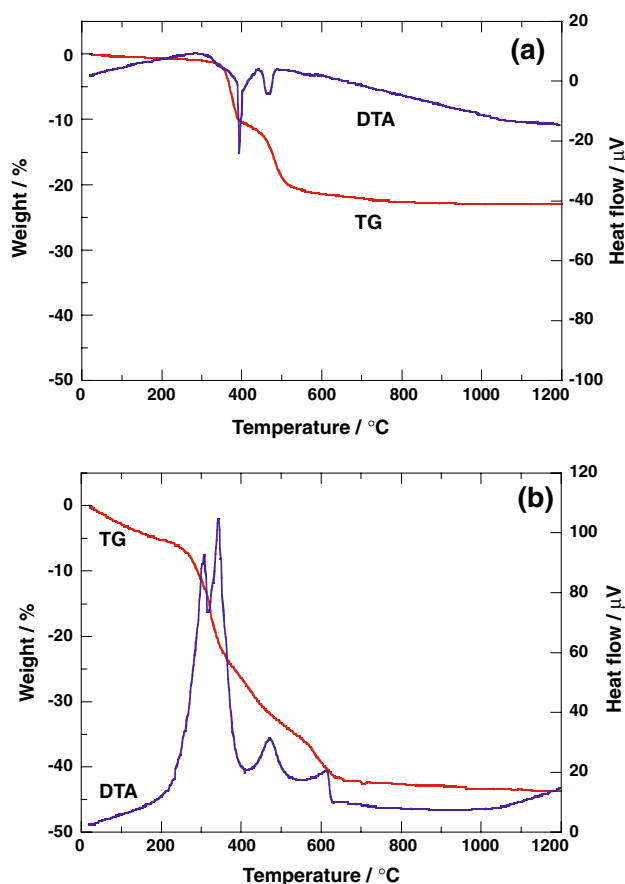


Fig. 2 TG-DTA analysis of the powders prepared by the solvothermal treatment of in (a) water and (b) ethylene glycol at 250 °C for 5 h

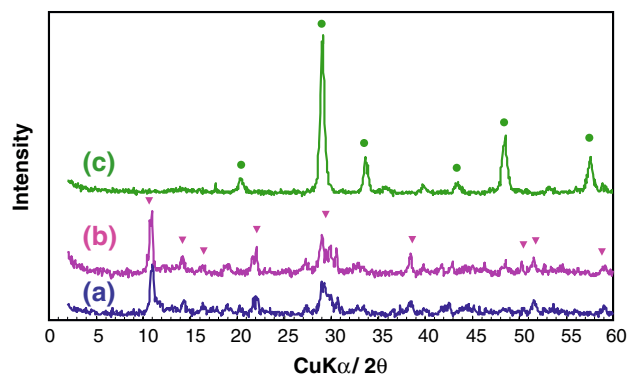


Fig. 3 XRD patterns of the powders prepared by (a) hydrothermal treatment at 250 °C for 5 h, and calcined sample (a) in air at (b) 550 °C, and (c) 800 °C. ▼: $Y_4O(OH)_9(NO_3)$; ○: Y_2O_3

multi-peaks might be related to the strongly adsorbed ethylene glycol, which might be burned out step-by-step during the TG-DTA measurement. The CHN elements analysis data also agreed with the calculated values for $Y_4O(OH)_9(NO_3)$.

Figure 3 shows the XRD patterns of the powders prepared by hydrothermal treatment at 250 °C, then calcined the sample at various temperatures. The $Y_4O(OH)_9(NO_3):Eu$ changed to $Y_2O_3:Eu$ at above 550 °C. It is obvious that the peak intensity, i.e., crystallinity of Y_2O_3 , increased with increasing the calcination temperature. The products prepared in other solvents also showed the same behaviors. This data also agreed well with that of Fig. 2.

Figure 4 shows the TEM photographs of the powders prepared by solvothermal treatments in various solvents. The powders prepared by the hydrothermal treatment

Fig. 4 TEM images of the $Y_4O(OH)_9(NO_3):Eu(3\%)$ powders prepared by solvothermal treatment in (a) water [AQ], (b) ethanol [EtOH], (c) 1-propanol [PrOH], (d) 1-butanol [BuOH], (e) ethylene glycol [EG], (f) 1,3-propanediol [1,3-PG], (g) 1,5-propanediol [1,5-PG], (h) 1,6-hexanediol [1,6-HG], and (i) polyethylene glycol 200 [PEG] at 250 °C for 5 h

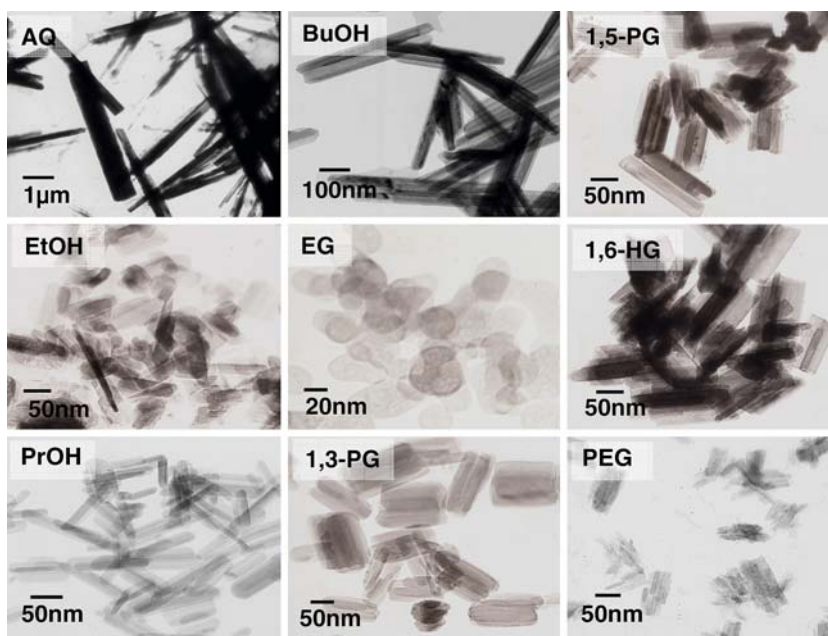


Table 1 Aspect ratio of the samples prepared by the solvothermal treatment

Solvent	Aspect ratio
Water [AQ]	12.3
Ethanol [EtOH]	4.8
1-Propanol [PrOH]	15.0
1-Butanol [BuOH]	15.1
Ethylene glycol [EG]	1.2
1,3-Propanediol [1,3-PG]	4.4
1,5-Pentanediol [1,5-PG]	6.2
1,6-Hexanediol [1,6-HG]	5.7
Polyethylene glycol 200 [PEG]	3.0

possessed wire-like morphology with large aspect ratio. The powders prepared by solvothermal treatments in alcohols such as ethanol (EtOH), 1-propanol (PrOH), and 1-butanol (BuOH) also showed wire-like structure, but the aspect ratio was lower than that in water. The powders prepared by solvothermal treatments in glycol solvents such as 1,2-propanediol (1,2-PG), 1,3-propanediol (1,3-PG), 1,3-butanediol (1,3-BG), 1,4-butanediol (1,4-BG), 1,5-propanediol (1,5-PG), 1,6-hexanediol (1,6-HG), and polyethylene glycol 200 (PEG) showed rod-like morphologies with much lower aspect ratio. On the other hand, the powders prepared in ethylene glycol (EG) showed a spherical-like morphology. The aspect ratio of the samples prepared by solvothermal treatment were summarized in Table 1. It is obvious that the samples obtained in aqueous and some alcohol solutions possessed such large aspect

ratio as 12–15; while those prepared in glycol type solvents showed comparatively smaller aspect ratio.

Figure 5 shows the TEM images of the $Y_2O_3:Eu(3\%)$ powders prepared by solvothermal treatment in various solvents followed by calcination at 1,200 °C. Compared with those in Fig. 4, it is obvious that the similar morphologies of the powders were kept even after calcinations at such high temperature as 1,200 °C.

Table 2 summarized some physical properties [18] of the solvents used in the present research. It is obvious that these solvents possessed different boiling point, viscosity, dielectric constant, and thermal conductivity. The powders treated in water prefer to form large particle size and high quality crystals. The high dielectric constant, high thermal conductivity, and low viscosity led to the high solubility and diffusion rate of ions in the solution, as a result, well-crystallized wire-like particles with large aspect ratio was produced. On the other hand, in the case of using high viscosity solvent such as glycols solvents, because of the low diffusion rate of ions in the solvent, crystalline growth was suppressed, and led to the formation of fine spherical nanoparticles. Similarly, in our previous reports [12, 16, 19], it was also found that the powders prepared in organic solvents showed softer agglomeration state and smaller crystalline size than those in water.

Figure 6 shows the effect of solvents on the emission spectra of $Y_2O_3:Eu(3 \text{ mol.}\%)$ particles with different morphologies. The samples were prepared by solvothermal treatment followed by calcination at 1,200 °C. The emission spectra at 612 nm are assigned to the $^5D_0 \rightarrow ^7F_2$

Fig. 5 TEM images of the $Y_2O_3:Eu(3\%)$ powders prepared by solvothermal treatment in (a) water [AQ], (b) ethanol [EtOH], (c) 1-propanol [PrOH], (d) ethylene glycol [EG], (e) 1,3-propanediol [1,3-PG], (f) 1,3-butanediol [1,3-BG], (g) 1,4-butanediol [1,4-BG], (h) 1,5-propanediol [1,5-PG], and (i) polyethylene glycol 200 [PEG] at 250 °C for 5 h, followed by calcination in air at 1,200 °C

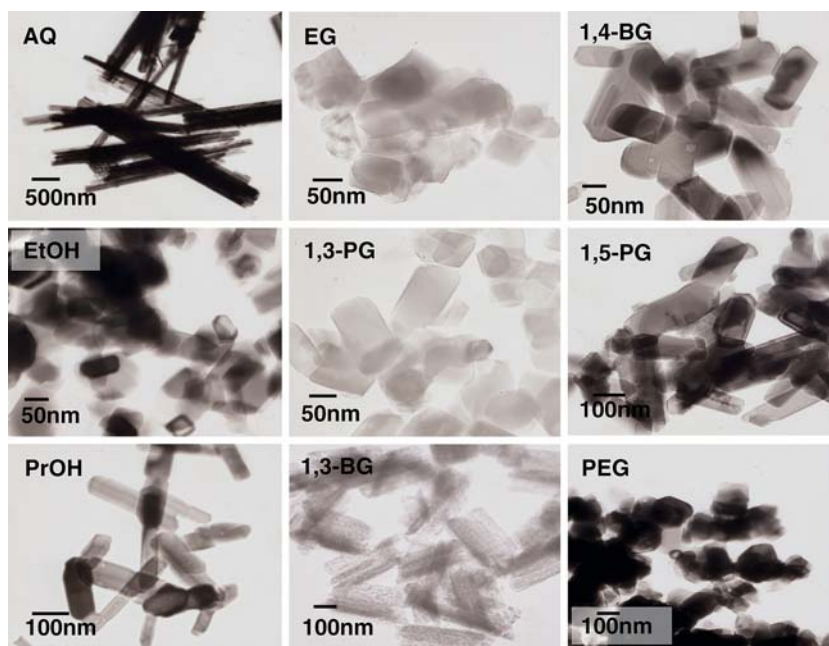


Table 2 Physical properties of the solvents utilized in the present research

Solvent	B.p., °C	Viscosity (25 °C), μPas	Dielectric constant (20 °C)	Thermal conductivity (25 °C), $\text{W m}^{-1} \text{K}^{-1}$
Water [AQ]	100	0.890	80.1	0.607
Ethanol [EtOH]	78.2	1.074	25.3	0.169
1-Propanol [PrOH]	97.2	0.321	20.8	0.154
1-Butanol [BuOH]	117.7	2.544	17.8	0.154
Ethylene glycol [EG]	197.8	16.1	41.4	0.256
1,2-Propanediol [1,2-PG]	187.6	40.4	27.5	–
1,3-Propanediol [1,3-PG]	214.4	–	35.1	–
1,3-Butanediol [1,3-BG]	207.5	–	28.8	–
1,4-Butanediol [1,4-BG]	235	–	1.9	–
1,5-Pentanediol [1,5-PG]	239	–	26.2	–
1,6-Hexanediol [1,6-HG]	208	–	25.86	–
Polyethylene glycol 200 [PEG]				

transition of Eu^{3+} ion [20]. Although the $\text{Y}_2\text{O}_3:\text{Eu}$ (3 mol.%) particles showed different morphologies and smaller particle sizes, the samples prepared in glycol solvents showed higher intensity than those prepared in water and alcohols.

Figure 7 shows the effect of calcination temperatures on the emission spectra of the $\text{Y}_2\text{O}_3:\text{Eu}$ (3 mol.%) prepared in ethylene glycol. The emission intensity at 612 nm increased with the calcination temperature, i.e., crystallinity of the $\text{Y}_2\text{O}_3:\text{Eu}$ (3 mol.%) particles. The samples prepared in other solvents also showed the same behavior. The TEM images in Fig. 5 indicated that the powders prepared by using ethylene glycol (EG) and other glycols showed soft agglomerates and near-spherical

morphologies. It is obvious that $\text{Y}_2\text{O}_3:\text{Eu}$ (3 mol.%) powders prepared in glycols possessed smaller particle size and about 1.2–1.6 times higher photoluminescence emission intensities than those prepared in water and alcohols.

Figure 8 shows the TEM images of various kinds of rare earth oxides powders prepared by hydrothermal and solvothermal treatment in ethylene glycol (EG) at 250 °C for 5 h. By the same synthesis manner as that of $\text{Y}_2\text{O}_3:\text{Eu}$ (3 mol.%) particles, it is very easy to prepare high aspect ratio wire-like or spherical particles nanoparticles of different kind of rare earth oxides such as Er_2O_3 , Nd_2O_3 , Ho_2O_3 , Lu_2O_3 , and Dy_2O_3 , although the aspect ratio or particle size changed somewhat depending on the kind of rare earth oxides.

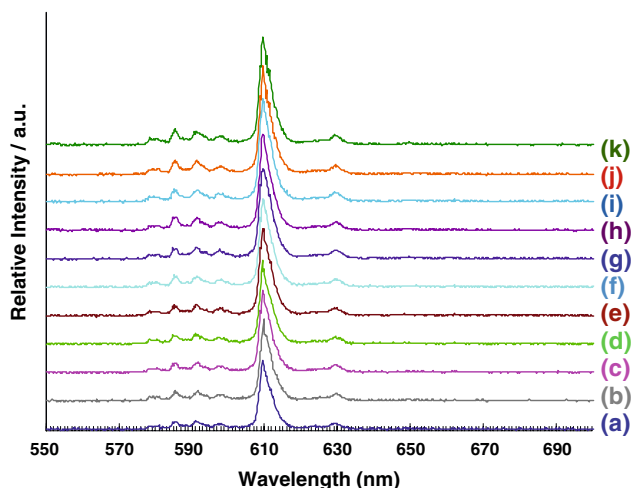


Fig. 6 Emission spectra of $\text{Y}_2\text{O}_3:\text{Eu}$ (3 mol.%) particles prepared by solvothermal treatment in (a) water [AQ], (b) 1-propanol [PrOH], (c) ethanol [EtOH], (d) 1,3-butanediol [1,3-BG], (e) 1,3-propanediol [1,3-PG], (f) 1-butanol [BuOH], (g) 1,4-butanediol [1,4-BG], (h) ethylene glycol [EG], (i) 1,5-propanediol [1,5-PG], (j) polyethylene glycol 200 [PEG], and (k) 1,6-hexanediol [1,6-HG] at 250 °C for 5 h, followed by calcination in air at 1,200 °C

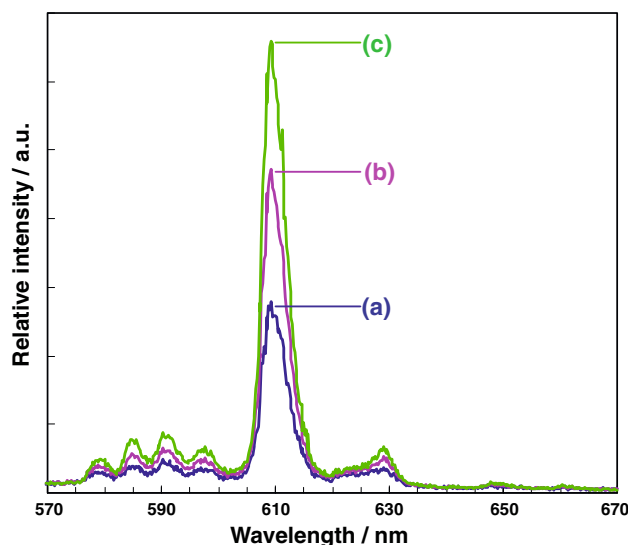


Fig. 7 Emission spectra of $\text{Y}_2\text{O}_3:\text{Eu}$ (3 mol.%) particles prepared by solvothermal treatment in ethylene glycol at 250 °C for 5 h followed by calcination at (a) 550, (b) 800, and (c) 1,200 °C for 1 h

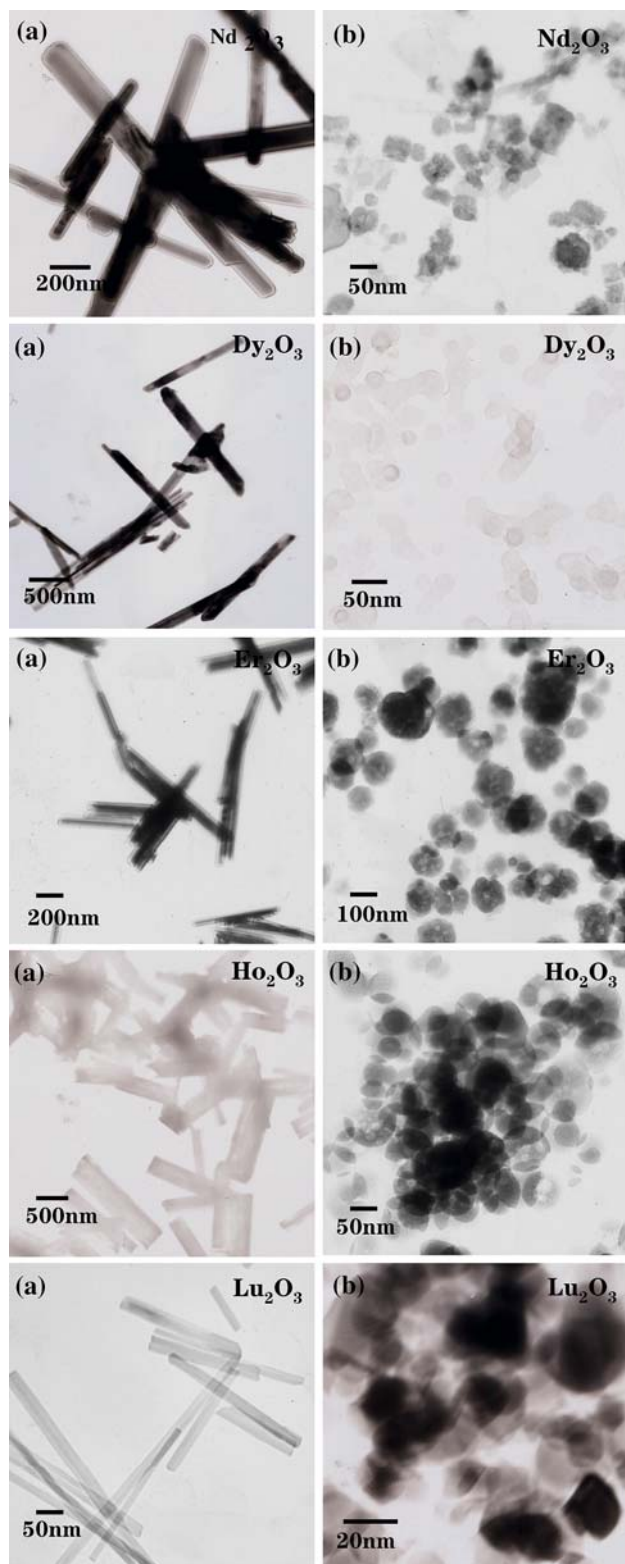


Fig. 8 TEM images of the rare earth oxides powders prepared by solvothermal treatment in (a) aqueous, and (b) ethylene glycol at 250 °C for 5 h, followed by calcination in air at 1,200 °C

Conclusions

Based on the above results, the following conclusions might be drawn:

1. $Y_2O_3:Eu(3 \text{ mol.}\%)$ wires and spherical-particles were successfully prepared by co-precipitation-solvothermal-calcination process using aqueous and ethylene glycol as solvothermal reaction media at 250 °C for 5 h.
2. High viscosity solvent led to the formation of near-spherical particles.
3. The near-spherical particles prepared by co-precipitation-solvothermal-calcination process using ethylene glycol showed almost the same photoluminescence emission level with the hardly agglomerated sub-micron particles by co-precipitation-calcination method.
4. Some other rare earth oxide nanoparticles such as Er_2O_3 , Nd_2O_3 , Ho_2O_3 , Lu_2O_3 , and Dy_2O_3 with wires and spherical morphologies could be prepared by the same manner.

Acknowledgements This research was carried out as a one of the projects in MSTECC Research Center at IMRAM, Tohoku University and partially supported by the Ministry of Education, Culture, Sports, Science and Technology, a Grant-in-Aid for the Scientific Research of Priority Areas (Panoscopic Assembling and High Ordered Functions for Rare Earth Materials).

References

1. Ronda CR (1997) *J Lumin* 72–74:49
2. Kang Y, Park S, Lenggoro I, Okuyama K (1999) *J Mater Res* 14:2611
3. Kang Y, Roh H, Park S (2000) *Adv Mater* 12:451
4. Sohn J, Kang Y, Park S (2002) *Jpn J Appl Phys* 14:3006
5. Wang L, Zhou Y, Quan Z, Lin J (2005) *Mater Lett* 59:1130
6. La R, Hu Z, Li H, Shang X, Yang Y (2004) *Mater Sci Eng A* 368:145
7. Zhang J, Hong G (2004) *J Solid State Chem* 177:1292
8. Hirai T, Asada Y, Komazawa I (2004) *J Colloid Interf Sci* 276:339
9. Lee M, Oh S, Yi S (2000) *J Colloid Interf Sci* 226:65
10. Vila L, Stucchi E, Davolos M (1997) *J Mater Chem* 7:2113
11. Piegza J, Zych E, Hreniak D, Strek W, Kepinski L (2004) *J Phys: Condens Mater* 16:6983
12. Yin S, Fujishiro Y, Sato T (1996) *Br Ceram Trans* 95:258
13. Yin S, Inoue Y, Uchida S, Fujishiro Y, Sato T (1998) *J Mater Res* 13:844
14. Yin S, Sato T (2000) *Ind Eng Chem Res* 39:4526
15. Wu J, Yin S, Lin Y, Lin J, Huang M, Sato T (2001) *J Mater Sci* 36:3055
16. Yin S, Aita Y, Komatsu M, Wang J, Tang Q, Sato T (2005) *J Mater Chem* 15:674
17. Yin S, Uchida S, Fujishiro Y, Aki M, Sato T (1999) *J Mater Chem* 9:1191
18. Lide D, Frederikse H (eds) (1995–1996) *CRC handbook of chemistry and physics*, 76th edn. CRC Press, Inc., New York, p 3-3, 6-159, 6-245, 6-253
19. Sato T, Inoue Y, Yin S, Fujishiro Y, Odashima T (1998) *Ceram Trans* 81:29
20. Silver J, Martinez-Rubio M, Ireland T, Fern G, Withnall R (2001) *J Phys Chem B* 105:9107